engineering proceedings

MDPI

Proceeding Paper

On-Chip Tests for the Characterization of the Mechanical Strength of Polysilicon †

Tiago Vicentini Ferreira do Valle [1,*], Aldo Ghisi [1], Stefano Mariani [1], Gabriele Gattere [2], Francesco Rizzini [2], Luca Guerinoni [2] and Luca Falorni [2]

[1] Department of Civil and Environmental Engineering, Politecnico di Milano, 20133 Milan, Italy
[2] AMS Group—R&D, STMicroelectronics, 20010 Cornaredo, Italy
* Correspondence: tiago.vicentini@polimi.it
† Presented at the 9th International Electronic Conference on Sensors and Applications, 1–15 November 2022; Available online: https://ecsa-9.sciforum.net/.

Abstract: Microelectromechanical systems (MEMS) are nowadays widespread in the sensor market, with several different applications. New production techniques and ever smaller device geometries require a continuous investigation of potential failure mechanisms in such devices. This work presents an experimental on-chip setup to assess the geometry- and material-dependent strength of stoppers adopted to limit the deformation of movable parts, using an electrostatically actuated device. A series of comb-finger and parallel plate capacitors are used to provide a rather large stroke to a shuttle, connected to the anchors through flexible springs. Upon application of a varying voltage, failure of stoppers of variable size is observed and confirmed by post-mortem ΔC–V curves. The results of the experimental campaign are collected to infer the stochastic property of the strength of polycrystalline, columnar silicon films.

Keywords: polysilicon tensile strength; polysilicon thin films; on-chip mechanical testing

Citation: do Valle, T.V.F.; Ghisi, A.; Mariani, S.; Gattere, G.; Rizzini, F.; Guerinoni, L.; Falorni, L. On-Chip Tests for the Characterization of the Mechanical Strength of Polysilicon. *Eng. Proc.* **2022**, *27*, 10. https://doi.org/10.3390/ecsa-9-13363

Academic Editor: Francisco Falcone

Published: 1 November 2022

1. Introduction

A large spectrum of microelectromechanical systems (MEMS) is characterized by a mechanical structure made of polycrystalline silicon films. Due to the columnar structure, the mechanical characterization of these films can be carried out using planar on-chip testing devices, see, e.g., [1–4]. Though they typically show a simple geometry, the relevant data reduction from actuation and read-out measures to mechanical indices does not always look simple, and the assessed elastic and strength properties of polysilicon often show a large scattering [5].

In the past, we have shown the importance of such materials-related data to understand the load-, or even the shock-carrying capacity of inertial devices [6,7]. Out of a multi-scale analysis, by considering all the features of the device falling, including the geometry at the package, die, movable structure, and structural film length-scales, we were able to correlate sensor failure and falling height [8]. It is thus of paramount importance to collect data relevant to the tensile strength of the (brittle) polysilicon films. Some results were already discussed in [9,10], but here we also investigate some additional features of the microfabrication process and their impact on the measured strength.

It should be noted that, in the case of bulky geometries of the movable frames, average values regarding the elastic and strength properties of silicon prove sufficient to design inertial MEMS. Moving in the direction of downscaling the footprint of each single device, the aforementioned average values no longer provide enough accuracy, because the geometry of some structural parts, such as, e.g., the suspension springs, become comparable in size to silicon grains. This effect invalidates the principle of length–scale separation that allows homogenization at the scale of silicon grain aggregates to be adopted to avoid a

statistical analysis at the microscale [11–13]. Monte Carlo simulations were then adopted to assess the spreading of results linked to devices, which were all identical if not for the uncertainties of sources due to the microfabrication. To speed up such investigation, deep learning strategies were recently proposed in [14,15].

Even though the stochastic mechanical resistance of ThELMA polycrystalline silicon was already statically explored [16], these studies were mostly focused on in-plane fracture. In this paper, the out-of-plane mechanical resistance of polycrystalline stoppers is evaluated through an on-chip experimental setup, where electrostatic actuation is used to push a massive shuttle against the stopper until failure is induced.

2. Materials and Methods

The polycrystalline silicon MEMS device shown in Figure 1 was developed by ST Microelectronics in partnership with the Politecnico di Milano. The movable structure was produced with the ThELMA microfabrication process [9,10] and features a series of 60 parallel plate stators and 504 comb finger stators to properly actuate the shuttle, which is supported by two springs on each side. Each die supports four similar devices, which differ in the in-plane size of the stopper, whose geometry is depicted in the inset of Figure 1; see also Figure 2. These in-plane dimensions were changed to assess the potential geometry-dependence of the polysilicon strength, still keeping the resistance of the stopper to the electro-static actuation minimal in compliance with the available microfabrication process.

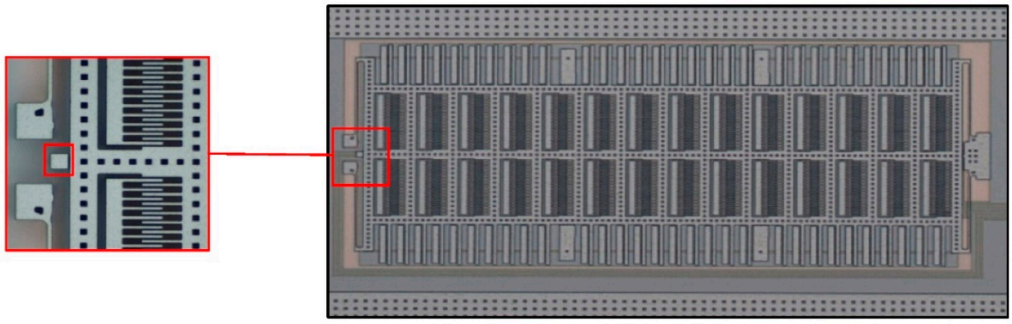

Figure 1. Picture of the device used in the experimental campaign. Inset on the left shows detail of the stopper.

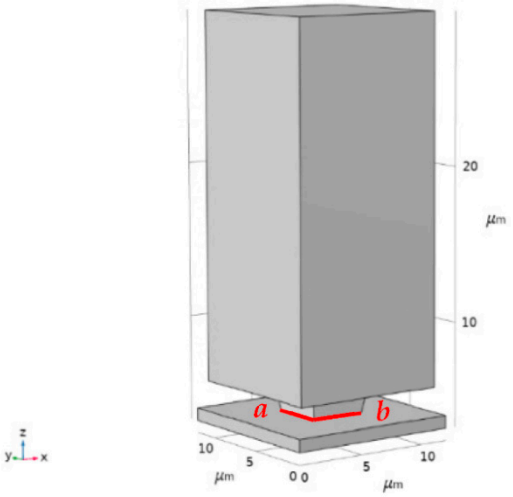

Figure 2. Geometry of the stopper; dimensions *a* and *b* at the base of the columnar structure can vary and are explicitly reported in Table 1.

Table 1. Experimental results, in terms of applied voltage, applied force, and computed tensile strength. For each experiment, nominal stopper sizes are also reported.

Test #	Stopper Dimensions (a μm × b μm)	φ_f (V)	Force at Failure (mN)	Nominal Tensile Strength (GPa)
1	3.9 × 4.4	196	4.78	0.77
2	3.9 × 4.9	208	5.37	0.78
3	3.9 × 4.9	219	5.94	0.86
4	3.9 × 4.4	211	5.52	0.89
5	3.9 × 4.4	211.5	5.55	0.90
6	3.9 × 4.9	225	6.26	0.91
7	3.9 × 4.9	230	6.54	0.95
8	3.9 × 3.9	213.5	5.65	1.03
9	3.9 × 3.9	218	5.89	1.07
10	3.9 × 3.9	219	5.94	1.08
11	3.9 × 3.9	232.5	6.68	1.22

The laboratory setup to actuate the shuttle and to measure the response to such actuation included an optical microscope equipped with micromanipulators, an Agilent E4980A capacitance meter, two digital 6614C Agilent DC power supplies, and an analogic DC power supply. The equipment was controlled from remote via a MATLAB code. The capacitance meter was connected to the comb fingers to read the change in capacitance and to apply voltage to the actuator until a maximum value of 40 V. The DC power supplies were instead connected in series to provide a maximum actuation of 250 V to the parallel plate stators. During the experiments, we first applied a voltage, both to the comb fingers and to the parallel plates pushing the shuttle against the stopper; next, the voltage at the parallel plates was raised until stopper failure. While voltage was applied, the capacitance meter read the change in capacitance induced at the comb fingers, to indirectly measure the motion of the entire shuttle.

The general procedure used throughout the experiments was subdivided into stages as follows:

1. Pre-mortem ΔC–V curves were obtained by means of a voltage up to 40 V applied on the comb fingers with steps of 0.5 V, and with the relevant capacitance change measured at each step.
2. The same 40 V voltage was applied to the comb fingers through the capacitance meter, then voltage was applied instead to the parallel plates by the three DC power supplies in series up to 250 V.
3. A post-mortem ΔC–V curve was obtained by solely using the capacitance meter, similarly to the first step.

The objectives of these stages were as follows, respectively: to check whether the stopper structure was initially pristine in the device, which could be linked to a constant value of the capacitance as soon as the stopper was touched by the shuttle; to cause a failure of the stopper; to perform a check whether the stopper was still able to resist mechanical stress or if it was completely broken. Special attention was paid to the current limitation, set to 3 mA as a maximum in every experiment, to avoid heating and possible thermally-induced loss of integrity of the MEMS structure.

3. Results

A series of experiments was performed in accordance with the above-described procedure, yielding failures as proven by the post-mortem ΔC–V curves. In these experiments, the applied voltage causing the failure was the main parameter to be assessed, thanks to the pull-in phenomenon observed in the ΔC–V curve or to a sudden significant change in the capacitance. These occurrences in the capacitance response curve were observed on the order between 1000 fF and 3500 fF.

To move from the voltage at failure to the electrostatic force, and then to the failure strength, some assumptions were made to simplify the coupled electromechanical problem. As shown in [17], the polysilicon springs that support the shuttle provide a reaction in the order of 70 μN for a displacement of 1.4 μm of the structure (distance needed by the shuttle to touch the stopper). Because the forces provided by the electrostatic actuators were in the order of 10 mN in the same state, the formerly mentioned spring reactions were disregarded. The aforementioned travel distance also accounted for the over-etch, caused by the microfabrication process; see [3,18–21].

The force provided by the comb fingers and the parallel plates are respectively given by, see e.g., [22]:

$$F_{PP} = N_{PP}\frac{\epsilon Bl}{2}\left(\frac{\varphi}{d_{PP}}\right)^2, \quad (1)$$

$$F_{CF} = N_{CF}\frac{\epsilon B}{d_{CF}}\,\varphi^2, \quad (2)$$

where F_{PP} is the total force at the parallel plate capacitors, while F_{CF} is the total force at the comb finger capacitors; ϵ is the dielectric permittivity of the medium, approximately assumed to be the vacuum one because of the low pressure inside the encapsulated device; B is the shuttle and stopper thickness; l is the length of one parallel plate; φ is the applied voltage; d_{PP} and d_{CF} are, respectively, the distances between the parallel plates (equal to the final displacement of the shuttle, when it touches the stopper) and the lateral distance between the comb fingers; N_{PP} is the number of parallel plate actuators; and N_{CF} is the number of comb fingers.

As the finger actuators were charged with 40 V in every case, the force contribution was the same in all experiments, amounting to around $F_{CF} = 107$ μN. As regards the parallel plates force, it varies with the voltage, φ, as shown in Figure 3.

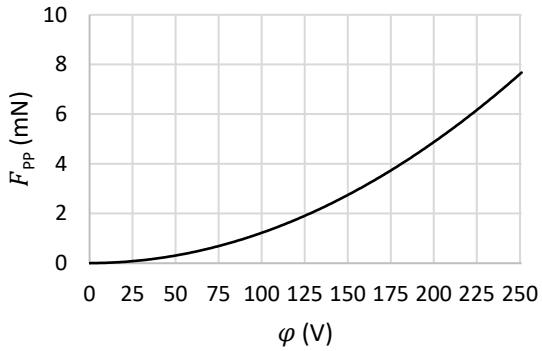

Figure 3. Theoretical relation between the applied voltage, φ, in the parallel plates and the correspondent force, F_{PP}.

.

To determine the sample tensile strength, only small deformations were considered in the model. The contact force applied to the stopper was assumed to be concentrated at the bottom of the contact area. A stress analysis was then performed at the bottom of the stopper, where the moment reached its maximum value. By assuming a pure deflection of the stopper, the maximum value of the out-of-plane tensile stress reads:

$$\sigma(a/2) = \frac{a}{2}\cdot\left[\left(\frac{h}{I}\right)\left(N_{CF}\frac{\epsilon Bl}{2}\left(\frac{\varphi_f}{d_{PP}}\right)^2 + N_{CF}\frac{\epsilon B}{d_{CF}}\,(40V)^2\right)\right], \quad (3)$$

where I is the moment of inertia of the stopper cross-section; h is the height of the column, which acts as the lever arm for the moment; and φ_f is the voltage applied to the parallel plates at failure. In Table 1, data are collected for some of the experiments performed, showing the value of the applied voltage on the parallel plates at rupture, the corresponding

electrostatic force, and the maximum stress at the base, as computed through Equation (3). In Figure 4, the cumulative probability distribution of the tensile strength of the tested polysilicon film samples is shown, as arrived at via Equation (3).

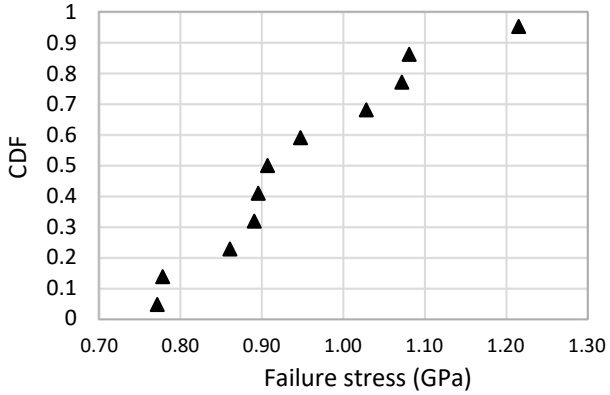

Figure 4. Cumulative distribution function (CDF) curve of polysilicon strength, as obtained with the present experimental campaign.

4. Discussion

Because these are preliminary results of an on-going experimental campaign, it is too early to infer a statistically significant strength for ThELMA polysilicon at the stoppers. We can mention that the values ranging from 0.77 GPa to 1.22 GPa were not too far from other experimental works, such as [23], but they were underestimated compared to typical ST Microelectronics MEMS; see, e.g., the study reported in [24]. However, the mentioned values were obtained from a simple formula based on the strength of material theory and neglected the stress intensification factor, which was evaluated by a finite element analysis as being $k = 3.6$. Thus, a tensile strength correction of $\tilde{\sigma} = k\sigma$ could be adopted, leading to experimental values in the range of 2.78–4.38 GPa, in line with previous works [23,24].

As for a brittle material, typically a Weibull distribution [25] should be adopted; in this distribution, the role of the defects is accounted for, because the larger the considered area/volume, the higher the probability to find a flaw and the lower the apparent resistance. Hence, it is worth emphasizing that, because in this study we were considering three different nominal geometries, with different sizes under the same loading conditions, coherently different strengths appeared, as shown in Figure 4 and Table 1. Slightly larger values were visible for the smaller 3.9×3.9 μm^2 device (tests #8–11), and intermediate values for the 3.9×4.4 μm^2 and the 3.9×4.9 μm^2 devices (tests #1–7), whose section dimensions provided larger areas.

5. Conclusions

We proposed a newly designed on-chip testing device for the characterization of the polysilicon films of MEMS movable structures. The device featured a compliant mechanism that allowed a massive shuttle to largely move and provide loading to a stopper, whose failure can be used to infer the mechanical strength of polysilicon. The different in-plane dimensions of the said stopper gave us the capability to also collect information concerning the size- and geometry-dependence of the strength properties.

Some results of the experimental campaign carried out with this device were collected. Even though outcomes were still partial, as testified by sharp transitions in the probability distribution curve adopted to report the results, the capability and usefulness of the designed testing device looks encouraging for the mechanical characterization of polysilicon films within a truly stochastic framework.

Author Contributions: Conceptualization, A.G. and T.V.F.d.V.; methodology, T.V.F.d.V.; software, T.V.F.d.V.; validation, A.G. and S.M.; formal analysis, A.G. and T.V.F.d.V.; investigation, A.G. and T.V.F.d.V.; resources, G.G., F.R., L.G. and L.F.; data curation, A.G. and T.V.F.d.V. writing—original draft preparation, TT.V.F.d.V. and A.G.; writing—review and editing, S.M.; visualization, S.M.; supervision, S.M. and A.G.; project administration, S.M.; funding acquisition, S.M. and A.G. All authors have read and agreed to the published version of the manuscript.

Funding: This research was funded by STMicroelectronics through project *Reliable-MEMS*.

Institutional Review Board Statement: Not applicable.

Informed Consent Statement: Not applicable.

Data Availability Statement: The data presented in this study are available on request from the corresponding author. The data are not publicly available due to some confidentiality issues.

Acknowledgments: Authors are indebted to Matteo Furlan for his support in developing the numerical models of the testing device.

Conflicts of Interest: The authors declare no conflict of interest.

References

1. Reedy, E.D.; Boyce, B.L.; Foulk, J.W.; Field, R.V.; de Boer, M.P.; Hazra, S.S. Predicting fracture in micrometer-scale polycrystalline silicon MEMS structures. *J. Microelectromech. Syst.* **2011**, *20*, 922–932. [CrossRef]
2. Vayrette, R.; Raskin, J.P.; Pardoen, T. On-chip fracture testing of freestanding nanoscale materials. *Eng. Fract. Mech.* **2015**, *150*, 222–238. [CrossRef]
3. Mirzazadeh, R.; Eftekhar Azam, S.; Mariani, S. Micromechanical characterization of polysilicon films through on-chip tests. *Sensors* **2016**, *16*, 1191. [CrossRef] [PubMed]
4. Mariani, S.; Ghisi, A.; Mirzazadeh, R.; Eftekhar Azam, S. On-Chip testing: A miniaturized lab to assess sub-micron uncertainties in polysilicon MEMS. *Micro Nanosyst.* **2018**, *10*, 84–93. [CrossRef]
5. Gravier, S.; Coulombier, M.; Sa, A.; Andr, N.; Bo, A.; Raskin, J.-P.; Pardoen, T. New on-chip nanomechanical testing laboratory—Applications to aluminum and polysilicon thin fims. *J. Microelectromech. Syst.* **2009**, *18*, 555–569. [CrossRef]
6. Mariani, S.; Ghisi, A.; Fachin, F.; Cacchione, F.; Corigliano, A.; Zerbini, S. A three-scale FE approach to reliability analysis of MEMS sensors subject to impacts. *Meccanica* **2008**, *43*, 469–483. [CrossRef]
7. Mariani, S.; Ghisi, A.; Corigliano, A.; Zerbini, S. Modeling impact-induced failure of polysilicon MEMS: A multi-scale approach. *Sensors* **2009**, *9*, 556–567. [CrossRef]
8. Ghisi, A.; Fachin, F.; Mariani, S.; Zerbini, S. Multi-scale analysis of polysilicon MEMS sensors subject to accidental drops: Effect of packaging. *Microelectron. Reliab.* **2009**, *49*, 340–349. [CrossRef]
9. Corigliano, A.; De Masi, B.; Frangi, A.; Comi, C.; Villa, A.; Marchi, M. Mechanical characterization of polysilicon through on-chip tensile tests. *J. Microelectromech. Syst.* **2004**, *13*, 200–219. [CrossRef]
10. Corigliano, A.; Ghisi, A.; Langfelder, G.; Longoni, A.; Zaraga, F.; Merassi, A. A microsystem for the fracture characterization of polysilicon at the micro-scale. *Eur. J. Mech. A/Solids* **2011**, *30*, 127–136. [CrossRef]
11. Mullen, R.; Ballarini, R.; Yin, Y.; Heuer, A. Monte Carlo simulation of effective elastic constants of polycrystalline thin films. *Acta Mater.* **1997**, *45*, 2247–2255. [CrossRef]
12. Mariani, S.; Martini, R.; Ghisi, A.; Corigliano, A.; Simoni, B. Monte Carlo simulation of micro-cracking in polysilicon MEMS exposed to shocks. *Int. J. Fract.* **2011**, *167*, 83–101. [CrossRef]
13. Mariani, S.; Martini, R.; Ghisi, A.; Corigliano, A.; Beghi, M. Overall elastic properties of polysilicon films: A statistical investigation of the effects of polycrystal morphology. *Int. J. Multiscale Comput. Eng.* **2011**, *9*, 327–346. [CrossRef]
14. Mariani, S.; Quesada Molina, J.P. A two-scale multi-physics deep learning model for smart MEMS sensors. *J. Mater. Sci. Chem. Eng.* **2021**, *9*, 41–52.
15. Quesada Molina, J.P.; Mariani, S. Hybrid model-based and data-driven solution for uncertainty quantification at the microscale. *Micro Nanosyst.* **2022**, *14*, 281–286.
16. Langfelder, G.; Longoni, A.; Zaraga, F.; Corigliano, A.; Ghisi, A.; Merassi, A. A polysilicon test structure for fatigue and fracture testing in micro electromechanical devices. In Proceedings of the IEEE SENSORS 2008, Lecce, Italy, 26–29 October 2008; pp. 94–97.
17. Furlan, M. Modelling Simulation and Design of Micro-Testing Machines For Microsystem Fracture Characterization. Master's Thesis, Politecnico di Milano, Milano, Italy, 2020.
18. Mirzazadeh, R.; Mariani, S. Uncertainty quantification of microstructure-governed properties of polysilicon MEMS. *Micromachines* **2017**, *8*, 248. [CrossRef]
19. Mirzazadeh, R.; Ghisi, A.; Mariani, S. Statistical investigation of the mechanical and geometrical properties of polysilicon films through on-chip tests. *Micromachines* **2018**, *9*, 53. [CrossRef]
20. Mirzazadeh, R.; Eftekhar Azam, S.; Mariani, S. Mechanical Characterization of Polysilicon MEMS: A Hybrid TMCMC/POD-Kriging Approach. *Sensors* **2018**, *18*, 1234. [CrossRef]

21. Bagherinia, M.; Mariani, S. Stochastic Effects on the Dynamics of the Resonant Structure of a Lorentz Force MEMS Magnetometer. *Actuators* **2019**, *8*, 36. [CrossRef]
22. Corigliano, A.; Ardito, R.; Comi, C.; Frangi, A.; Ghisi, A.; Mariani, S. *Mechanics of Microsystems*; John Wiley & Sons: Chichester, UK, 2017.
23. Bagdahn, J.; Sharpe, W.N.; Jadaan, O. Fracture strength of polysilicon at stress concentrations. *J. Microelectromech. Syst.* **2003**, *12*, 302–312. [CrossRef]
24. Cacchione, F.; De Masi, B.; Corigliano, A.; Ferrera, M. Rupture tests on polysilicon films through on-chip electrostatic actuation. In Proceedings of the 5th International Conference on Thermal and Mechanical Simulation and Experiments in Microelectronics and Microsystems, Brussels, Belgium, 10–12 May 2004.
25. Boroch, R.; Wiaranowski, J.; Mueller-Fiedler, R.; Ebert, M.; Bagdahn, J. Characterization of strength properties of thin polycrystalline silicon films for MEMS applications. *Fatigue Fract. Eng. Mater. Struct.* **2007**, *30*, 2–12. [CrossRef]